ELSEVIER

Eur. J. Med. Chem. 37 (2002) 301–313

EUROPEAN JOURNAL OF MEDICINAL CHEMISTRY

www.elsevier.com/locate/ejmech

Original article

Synthesis, cytotoxic activities and proposed mode of binding of a series of bis{[(9-oxo-9,10-dihydroacridine-4-carbonyl)-amino]alkyl}alkylamines

Miguel F. Braña [a,*], Luis Casarrubios [a], Gema Domínguez [a], Carlos Fernández [a], José M. Pérez [b], Adoración G. Quiroga [b], Carmen Navarro-Ranninger [b], Beatriz de Pascual-Teresa [a]

[a] *Departamento de Química Orgánica y Farmacéutica, Facultad de Ciencias Experimentales y de la Salud, Universidad San Pablo CEU, Boadilla del Monte, E-28668 Madrid, Spain*

[b] *Departamento de Química Inorgánica, Universidad Autónoma de Madrid, E-28049 Madrid, Spain*

Received 11 November 2001; received in revised form 1 February 2002; accepted 8 February 2002

This paper is dedicated to the memory of Professor Joaquín de Pascual Teresa

Abstract

A series of bis{[(9-oxo-9,10-dihydroacridine-4-carbonyl)amino]alkyl}alkylamines have been prepared and their antiproliferative properties have been tested against HT-29 cell lines. Compounds **6b** and **6d** showed an interesting cytotoxic profile and were subjected to further cytotoxic evaluation, DNA binding properties and molecular modelling studies. The evaluation of the cytotoxic activity of compounds **6b** and **6d** against pairs of cisplatin-sensitive and -resistant ovarian tumour cells shows that both compounds may be endowed with interesting antitumour properties because they are able to circumvent cisplatin resistance in A2780cisR, CH1cisR and Pam 212-ras tumour cells. On the other hand, DNA binding data indicate that compounds **6b** and **6d** are able to intercalate stronger than acridine within the double helix. Both compounds displace ethidium bromide with an efficiency ten times higher than acridine from several linear double-stranded DNAs and induce 43° unwinding in supercoiled pBR322 DNA while acridine unwinds pBR322 DNA by only 24°. Altogether these data indicate that the significant conformational changes induced by compounds **6b** and **6d** in the double helix are due to a bis-intercalative DNA binding mode. We propose that binding to DNA through bisintercalation might be at least in part responsible for the remarkable cytotoxic properties of these acridine derivatives. The complex of **6b** with $d(GCGCGC)_2$ in the four possible orientations that the ligand can adopt when binding to the DNA hexamer have been modelled and subjected to molecular dynamics simulations with the aim of evaluating the binding preferences of this bisintercalating agent into the DNA molecule. The predictions suggest that **6b** binds to $d(GCGCGC)_2$ with a parallel orientation of the chromophores relative to each other and with a preference for binding through the minor groove of the hexamer. The possible relevance of these findings to the process of bisintercalation and the antitumour profile of these compounds is discussed in this paper.

Keywords: acridine; molecular modelling; bisintercalation; anticancer; DNA-binding; cytotoxicity

1. Introduction

Acridine based chemotherapeutic agents have a long history and include antimalarial, antibacterial and antitumour compounds. A number of agents from these classes have entered clinical use and several others are under intensive development by research groups throughout the world. These compounds have quite different ranges of biological activities and modes of action, but all have in common the ability to bind tightly but reversibly to DNA by intercalation between the base pairs of the double helix. In fact, the concept of intercalation was first introduced to explain the reversible and noncovalent binding of some acridines to DNA [1]. Interest in bifunctional intercalators

* Correspondence and reprints.
E-mail address: mfbrana@ceu.es (M.F. Braña).

0223-5234/02/$ - see front matter
PII: S0223-5234(02)01348-X

originally stemmed from the possibility of enhancing the binding constant over that of the corresponding monomers. The synthesis of these bifunctional intercalators was originally stimulated by the idea that the pharmacological activity of intercalating drugs could be enhanced by the significantly higher DNA binding constants and slower dissociation rates from DNA expected for bisintercalators relative to monointercalators. On the other hand, increasing the global size occupied by the ligand could afford greater opportunities for sequence selectivity. The bis(naphthalimide) LU79953 (elinafide) constitutes an excellent example of a bis-intercalator with a broad-spectrum activity against a variety of human solid tumour cell lines (both in culture and as xenographs in nude mice) [2–4], and is in Phase I clinical trials [5]. The synthesis and cytotoxic profile of a large amount of bisacridine derivatives has been extensively investigated by Denny et al. [6–9] and others [10,11].

We report here the synthesis of a new series of bisintercalators, consisting of two 9-oxo-9,10-dihydroacridine-4-carboxamide units joined by different cationic linkers. IC_{50} values against HT-29 cell lines were measured for all compounds, showing an antitumour profile strongly dependent on the nature of the linking chain and especially remarkable for compounds **6b** and **6d**. Additional cytotoxicity data show that in contrast with acridine, compounds **6b** and **6d** are able to circumvent cisplatin resistance in pairs of cisplatin-sensitive and -resistant cell lines [12]. On the other hand, fluorescent ethidium bromide displacement assays in calf thymus DNA and poly $[d(AT)_2]$ and poly $[d(GC)_2]$ oligodoxynucleotides indicate that both **6b** and **6d** bind ten times stronger than acridine to DNA. These results were supported by measurements of the unwinding angles induced by compounds **6b** and **6d** and acridine upon binding to open circular (oc) and covalently closed circular (ccc) forms of pBR322 DNA. In fact, while acridine induced an unwinding of 24° in pBR322 plasmid DNA, compounds **6b** and **6d** induced 43° unwinding suggesting that bis-intercalation of the chromophores induces significant conformational changes in the double helix.

Molecular models have proved to be very useful for understanding function of nucleic acids at the atomic level and detailed structural information about these macromolecules and their complexes with small ligands (e.g. DNA-binding drugs) is provided mostly by X-ray crystallography and nuclear magnetic resonance techniques. Although the amount of X-ray [13,14], modelling [15] and experimental [16] works devoted to the study of the mode of binding of monointercalating acridine derivatives to DNA is relevant, little is known about the mode of interaction of bisacridinecarboxamide derivatives to DNA. We show here a molecular dynamics study involving compound **6b** and the alternating hexanucleotide $d(GCGCGC)_2$, in which the ligand embraces the central GpC binding site. The sequence was selected according to the binding preference demonstrated for related monointercalating compounds [13,14]. Thus, the selected hexanucleotide contains three contiguous GpC sites, of which the central one is sandwiched by the drug chromophores. This study corroborates that this type of compound is able to form stable complexes with the DNA molecule through bisintercalation, and that it does that by locating both chromophores in a relative parallel orientation.

2. Chemistry

Fig. 1 shows the synthetic routes to 9-oxo-9,10-dihydroacridine-4-carboxylic acid (2-dimethylaminoethyl)-amides and to bis{[(9-oxo-9,10-dihydroacridine-4-carbonyl)amino]alkyl}alkylamines [17] shown in Table 1. Condensation of diphenyliodonium-2-carboxylate [18] with the corresponding methyl antranylates in DMF and in the presence of copper(II) acetate following the procedure previously described by Denny [19], ring closure using polyphosphoric ethyl ester and in situ hydrolysis with a 1M solution of sodium hydroxide in 50% aqueous ethanol, gave the 9-oxo-9,10-dihydroacridine-4-carboxylic acids **1** [19]. The extremely low solubility of these acids made impossible the reaction between the corresponding acid chloride and the bisamines. Activation of the acid with DCC, DCI and other coupling reagents was also unsuccessful. Treatment of the acids **1** with cyanuric fluoride (Alfa 13897) in anhydrous DMF according to the method described by Carpino [20], yielded the corresponding 9-oxo-9,10-dihydroacridine-4-carbonyl fluorides **2** which were used without further purification. The reaction of fluorides **2b**,**c** with 1.00 equivalent of *N*,*N*-dimethylethylenediamine allowed the obtention of monomers **7b**,**c** which were tested against HT-29 human colon line and the obtained activities (**7b**: 4.4×10^{-6} M, **7c**: 1.5×10^{-6} M) were taken as reference values when compared to the ones of compounds **3**–**6**. Treatment of fluorides **2** with different dialkylamines allowed the obtention of bis{[(9-oxo-9,10-dihydroacridine-4-carbonyl)amino]-alkyl}alkylamines **3**–**6**, shown in Table 1. Based on molecular modelling, best activities are expected for compounds where the two chromophore units are linked by a 12 or 13 atoms chain. To increase the number of structural changes, compounds **5d** and **6d** were synthesised by reduction of the nitro group in **5c** and **6c**, respectively (see Fig. 1). Thus, treatment of these compounds with hydrazine monohydrate in the presence of Raney–Ni in THF gave the 1-aminoderivatives **5d** and **6d** in excellent yields.

3. Cytotoxic activity

The structures of the bis-compounds prepared by the above methods are listed in Table 1 together with their cytotoxicities (as IC_{50} values) in HT-29 human colon line. Selected compounds (**6b** and **6d**) were also evaluated together with acridine, ethidium bromide and cisplatin against several tumour lines sensitive to cisplatin (A2780 and CH1), resistant to cisplatin (A2780cisR, CH1cisR and Pam 212-ras) and normal cells (Pam 212). Results are shown in Table 2 as IC_{50} values. It may be seen that **6b** exhibits IC_{50} values between 0.35 and 72 μM having a cytotoxic activity similar to that of **6d** that shows IC_{50} values between 0.20 and 74 μM. Table 2 also shows that compounds **6b** and **6d** are approximately 3.6-fold and 3.2-fold, respectively, more active than cisplatin in Pam 212-ras murine keratinocytes resistant to cisplatin (IC_{50} values of 20 and 22 μM, respectively, being the IC_{50} value of cisplatin of 72 μM). Interestingly, compounds **6b** and **6d** are able to circumvent acquired resistance to cisplatin in human ovarian tumour cell lines A2780cisR and CH1cisR (resistance factors defined as IC_{50} resistant line/IC_{50} parental line of 3.4, and 1.8 and of 3.7 and 2.0, respectively, versus 11.0 and 6.5 for cisplatin). On the other hand, the data of Tables 2 and 3 show that both acridine and ethidium

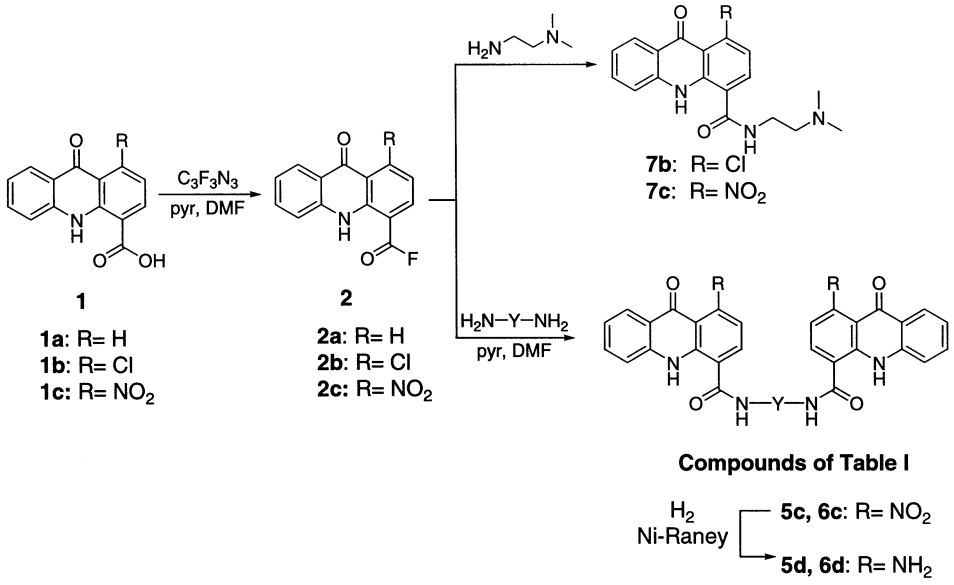

Fig. 1. Synthetic route for compounds **3**–**7**.

Table 1
Structures of synthesised bis{[(9-oxo-9,10-dihydroacridine-4-carbonyl)amino]alkyl}amines and cytotoxic activity in HT29 cells

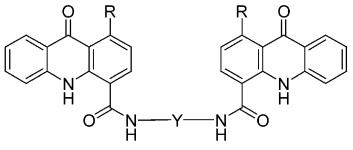

Compound	R	Y	IC_{50} (M) against HT-29 cells [a]
3b	Cl	$-(CH_2)_2-N(CH_3)-(CH_2)_2-$	1.4×10^{-6}
3c	NO_2	$-(CH_2)_2-N(CH_3)-(CH_2)_2-$	$>10^{-4}$
4b	Cl	$-(CH_2)_3-N(CH_3)-(CH_2)_3-$	2.3×10^{-6}
4c	NO_2	$-(CH_2)_3-N(CH_3)-(CH_2)_3-$	$>10^{-4}$
5b	Cl	$-(CH_2)_2-N(CH_3)-(CH_2)_2-N(CH_3)-(CH_2)_2-$	1.2×10^{-6}
5c	NO_2	$-(CH_2)_2-N(CH_3)-(CH_2)_2-N(CH_3)-(CH_2)_2-$	1.6×10^{-6}
5d	NH_2	$-(CH_2)_2-N(CH_3)-(CH_2)_2-N(CH_3)-(CH_2)_2-$	1.8×10^{-6}
6a	H	$-(CH_2)_2-N(CH_3)-(CH_2)_3-N(CH_3)-(CH_2)_2-$	5.0×10^{-7}
6b	Cl	$-(CH_2)_2-N(CH_3)-(CH_2)_3-N(CH_3)-(CH_2)_2-$	5.3×10^{-7}
6c	NO_2	$-(CH_2)_2-N(CH_3)-(CH_2)_3-N(CH_3)-(CH_2)_2-$	3.0×10^{-6}
6d	NH_2	$-(CH_2)_2-N(CH_3)-(CH_2)_3-N(CH_3)-(CH_2)_2-$	4.0×10^{-7}

[a] IC_{50} is the compound concentration (M) that inhibits cellular growth by a factor of 50%.

Table 2
IC_{50} mean values (μM) obtained for compounds ethidium, acridine, **6b**, **6d** and cisplatin against several human ovarian carcinoma cell lines and normal and transformed murine keratynocites

	IC_{50} (μM) ± SD [a] cell line panel					
	A2780	A2780cisR	CH1	CH1cisR	Pam 212	Pam 212-ras
Acridine	>10	>100	>10	>100	>200	>200
Ethidium	>10	>100	>10	>100	120 ± 6	180 ± 8 (1.5)
6b	0.35 ± 0.01	1.20 ± 0.20 (3.4)	0.40 ± 0.03	0.72 ± 0.04 (1.8)	72 ± 3	20 ± 3 (0.3)
6d	0.20 ± 0.02	0.74 ± 0.05 (3.7)	0.32 ± 0.04	0.64 ± 0.03 (2.0)	74 ± 4	22 ± 2 (0.3)
Cisplatin	0.30 ± 0.02	3.30 ± 0.05 (11)	0.10 ± 0.01	0.65 ± 0.05 (6.5)	44 ± 3	72 ± 4 (1.6)

[a] SD = standard deviation. Numbers in parentheses refer to resistance factors: IC_{50} resistant line/IC_{50} parent line.

bromide display a very low level of cytotoxic activity in all the cell lines tested.

4. DNA binding properties

4.1. Binding to double-stranded DNA

Fig. 2 shows the fluorescence quenching of ethidium bromide bound to calf thymus DNA (CT DNA) upon the addition of compounds **6b** and **6d** and acridine. The drug concentration needed to reduce the fluorescence of initially DNA-bound ethidium by 50% (C_{50} values) in CT DNA and in poly [d(AT)$_2$] and poly [d(GC)$_2$] oligodeoxynucleotides are shown in Table 2. The results of Fig. 2 suggest that quenching in fluorescence of CT DNA-bound ethidium is provoked by the displacement of ethidium from the double helix by intercalation of **6b** and **6d** and acridine. In addition, the C_{50} values of Table 2 show that binding to CT DNA and to poly [d(AT)$_2$] and poly [d(GC)$_2$] oligodeoxynucleotides of compounds **6b** and **6d** is about ten times stronger that that of acridine.

4.2. Binding to supercoiled DNA

Binding to DNA of compounds **6b** and **6d** was also studied on supercoiled DNA forms. We determined the ability of compounds **6b** and **6d** to alter the electrophoretic mobility of the ccc (covalently closed circular) and oc (open circular) forms of pBR322 plasmid DNA. Fig. 3 (panels A and B) shows the electrophoretic mobility of native pBR322 DNA and of pBR322 DNA incubated with compounds **6b** and **6d** (panel A) and acridine (panel B) at several molar ratios of intercalator per nucleotide (r). It has been reported that at increasing r, the rate of migration of the ccc DNA band decreases until it comigrates with the oc DNA band so that the molar ratio of drug/nucleotide at the coalescence point corresponds to the amount of intercalator molecules needed for complete removal of all supercoils from DNA [21]. The DNA unwinding angle, ϕ, can be calculated from the following equation [22]:

$$\phi = 18\sigma/r(c)$$

where σ is the superhelical density of the plasmid and $r(c)$ is the molar ratio of intercalator per nucleotide at the coalescence point. As can be seen in Fig. 3, the $r(c)$ value for compounds **6b** and **6d** was 0.025 (Panels B and C, lanes 6 and 7, respectively) that yield a ϕ value

Table 3
C_{50} mean values (μM) obtained for compounds **6b**, **6d** and acridine in the displacement assay of ethidium bound to calf thymus DNA, poly [d(AT)$_2$] and poly [d(GC)$_2$]

Compound	C_{50} [a] (μM) ± SD [b]		
	CT DNA [c]	poly [d(AT)$_2$]	poly [d(GC)$_2$]
6b	2.5 ± 0.2	5.3 ± 0.5	8.2 ± 0.9
6d	2.3 ± 0.2	5.4 ± 0.4	8.0 ± 0.7
Acridine	20 ± 1	60 ± 4	100 ± 6

[a] C_{50} is the compound concentration that reduces the fluorescence of initially DNA-bound ethidium by 50%.
[b] SD = standard deviation.
[c] CT DNA = calf thymus DNA.

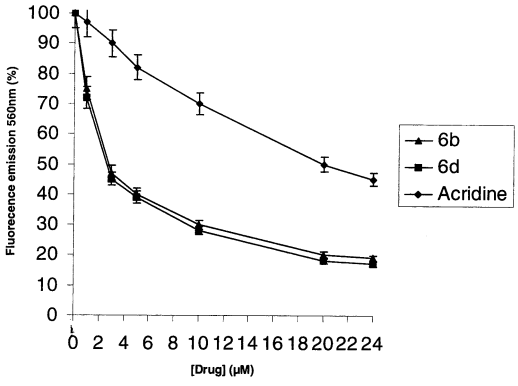

Fig. 2. Decrease in fluorescence of DNA-bound ethidium following addition of increasing μM concentrations of compounds **6b** (▲), **6d** (■) and acridine (●). [DNA] = 0.5 μM (base pairs), [ethidium] = 1.26 μM.

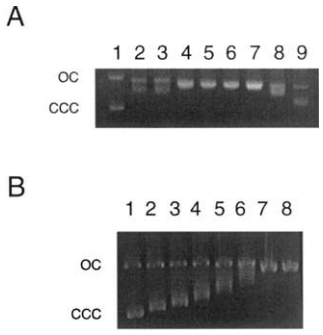

Fig. 3. Changes in electrophoretic mobility of the ccc (covalently closed circular) and oc (open circular) forms of pBR322 plasmid DNA modified at several molar ratios of drug/nucleotides (r) by compounds **6b**, **6d** and acridine. Panel (A) compounds **6b** and **6d**, respectively, at $r = 0.005$, (lanes 2 and 3); 0.010, (lanes 4 and 5); 0.025, (lanes 6 and 7); 0.030, (lanes 8 and 9); lane 1: control unmodified pUC8 DNA. Panel (B) acridine at $r = 0.01$ (lane 2); 0.10 (lane 3); 0.025 (lane 4); 0.03 (lane 5); 0.04 (lane 6); 0.045 (lane 7) and 0.05 (lane 8).

of $(43 \pm 2)°$ under our experimental conditions ($\sigma = -0.060$). For acridine, the calculated $r(c)$ value was 0.045 (Panel B; lane 7) which rendered a ϕ value of $(24 \pm 2)°$. The ϕ value of 24° obtained for acridine is close to the 26° ϕ value reported for ethidium under similar experimental conditions [23,24]. Because the ϕ value obtained for compounds **6b** and **6d** is 1.8 times higher than the ϕ value obtained for the mono-intercalator acridine it is most likely that the DNA binding mode of compounds **6b** and **6d** results from bis-intercalation.

5. Molecular modelling

Models were built for the complexes of **6d** with the hexanucleotide d(GCGCGC)$_2$ in the four possible

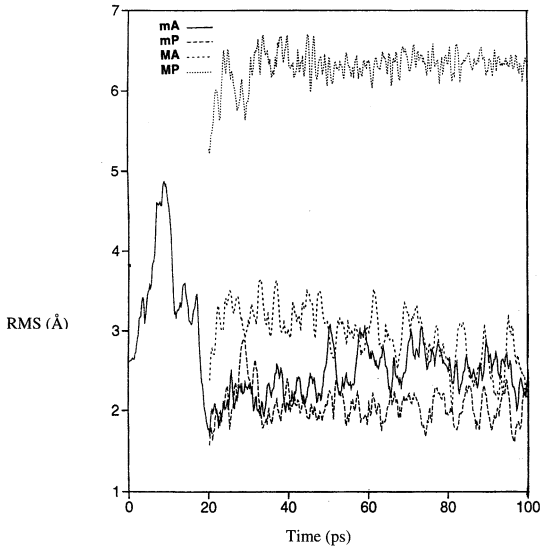

Fig. 5. Time evolution of the root-mean-square deviations from the initial structures, calculated for all non-hydrogen atoms after least-square fitting of the structures using the same atoms. From the dynamics simulations along the 80 ps sampling time for complexes **MA** (short dashed line), **MP** (dashed line) and **mP** (dotted line) and along the entire simulation time (100 ps) for complex **mA** (line).

orientations that the ligand can adopt when binding to DNA through a bisintercalation process. These orientations are shown schematically in Fig. 4. Among these four orientations there are two in which the ligand binds through the major groove of the DNA hexamer and differ in the relative orientation of the chromophores, that can be either parallel or antiparallel, denoted **MP** and **MA**, respectively. The same accounts for the minor groove binding models, denoted **mP** and **mA**.

Both the total potential energy of the systems (data not shown) and the root-mean-square deviation (Fig. 5) of the hexamer complexes with respect to the initial structures were evaluated for all four complexes. These

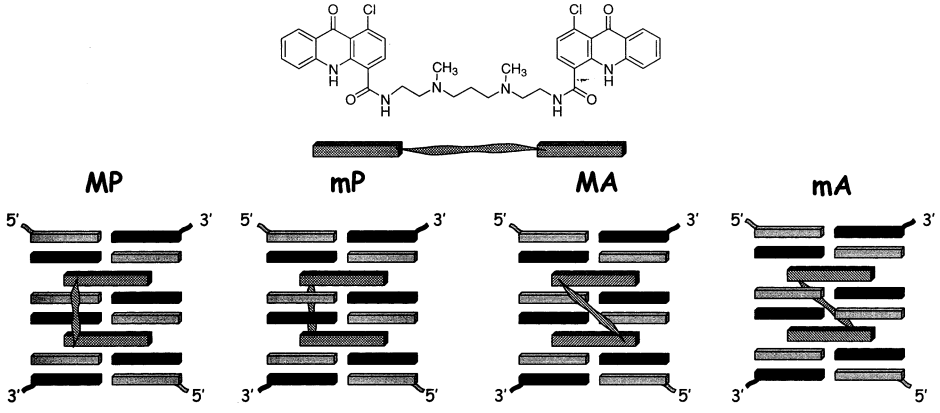

Fig. 4. Schematic view from the major groove of the four complexes between compound **6d** and a DNA hexamer containing the canonical CpG binding site. Black = guanine; gray = cytosine; checkerboard = compound **6d**. Left: Complexes with the ligand bound with the chromophores in a parallel orientation and bound through the major **MP** and minor groove **mP** of the DNA hexamer. Right: Complexes with the ligand bound with the chromophores in an antiparallel orientation and bound through the major **MA** and minor groove **mA** of the DNA hexamer.

values remained stable for complexes **MP**, **mP** and **mA**, whereas **MA** was markedly unstable. The progression of these two parameters indicates that the DNA:ligand complexes do not experience large conformational changes during the sampling time and thus can be considered to be in a state near equilibrium.

A visual inspection of an energy-minimised average structure from the 80–100 ps period of the molecular dynamics simulation for complexes **mP** and **mA** showed that in both complexes the ligand was in a similar orientation. These results prompted us, first to revise the initial conformation of both complexes and once we were certain that the models were correctly built, we proceeded to repeat the simulation for complex **mA** under the same conditions with the only exception that system coordinates were saved every 0.2 ps during the entire period of the simulation time and not only for the last 80 ps sampling period as described in the general methods. A detailed visualisation of the dynamics trajectory showed striking conformational changes that within the first 20 ps of the heating and equilibration periods of the dynamics simulation for **mA** inverted the relative orientation of the chromophores from an antiparallel to a parallel orientation. The time evolution of the first 20 ps of the molecular dynamics simulation for **mA** is depicted with detail in Fig. 6. Root-mean-square deviation for the entire simulation of **mA** is represented in Fig. 5. This value remained stable once the initial (20 ps) conformational changes had taken place, indicating that the resulting complex does not experience large conformational changes during the remaining time (80 ps) and thus can be considered to be in a state near equilibrium.

6. Results and discussion

We report here the synthesis, characterisation, cytotoxic activity and DNA binding properties of a series of bis-intercalators consisting of two 9-oxo-9,10-dihydroacridine-4-carboxamide units joined by different biscationic linkers. IC_{50} values against the HT29 cell line were determined for all the compounds, showing in most cases an interesting antitumour profile. Compounds **6b** and **6d** showed a marked cytotoxic activity against HT-29 colon cell lines and were selected for further biological and DNA binding assays. Compounds **6b** and **6d** are able to circumvent acquired resistance to cisplatin in the human ovarian tumour cell lines A2780cisR and CH1cisR. Due to the fact that CH1cisR cells are primarily resistant to *cis*-DDP through enhanced DNA repair/tolerance [25], the better resistance factors shown by compounds **6b** and **6d** in relation to cisplatin against these cell lines indicate that the DNA complexes formed by both compounds are different from those formed by *cis*-DDP. However, the possibility cannot be ruled out that in the pair of cell lines CH1/CH1cisR the existence of better resistance factors for compounds **6b** and **6d** relative to *cis*-DDP may be related to the fact that both bis-intercalators are slightly less active than *cis*-DDP against *cis*-DDP-sensitive CH1 cells. Thus, their overall cytotoxic activity could not be much higher than that of *cis*-DDP. On the other hand, the data of Table 2 show that both acridine and ethidium display a much lower level of cytotoxic activity than **6b** and **6d**. Interestingly, the lack of significant cytotoxic activity of acridine against CH1cisR cells suggests that the DNA adducts formed by this intercalator are efficiently repaired in this particular tumour cell line. However, the inactivity of acridine may also be due to its poor membrane permeability as it has been found in HeLa cells [12]. It has been previously reported that Pam 212-*ras* cells are resistant to *cis*-DDP ($>50\%$) when compared to the parental line Pam 212 [23]. Our findings agree with this observation and show the Pam 212-*ras* cells to be 64% less sensitive to *cis*-DDP than the parental line. The Pam 212-*ras* line has been reported to be also resistant ($>25\%$) to doxorubicin [22]. Like doxorubicin, compounds **6b** and **6d** are DNA intercalators [25]. However, the Pam 212-*ras* cells

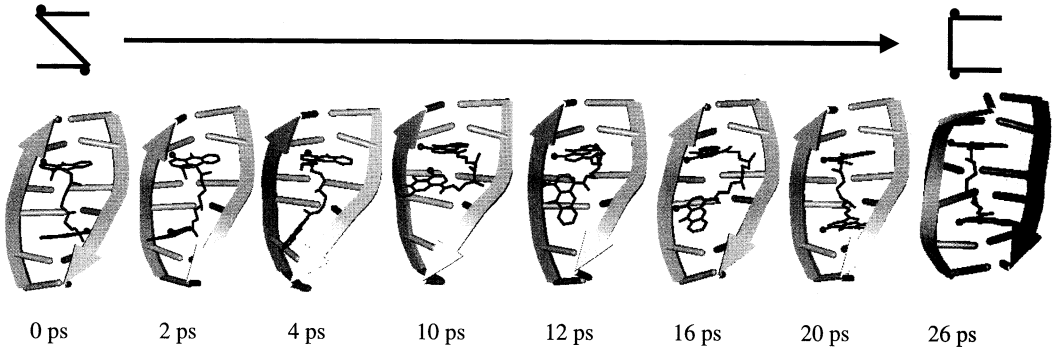

Fig. 6. Evolution of the trajectory of the first 26 ps of the molecular dynamics simulation of complex **mA**. The DNA hexamer is displayed as a ladder, while the ligand is displayed in sticks. Chlorine atoms are represented in balls. Hydrogens are omitted for clarity. The inverted Z indicates an antiparallel orientation of the drug chromophores, while the C stands for a parallel orientation.

were 70% less resistant than Pam 212 cells to both **6b** and **6d** (see Table 1). Interestingly, compounds **6b** and **6d** were more active against the Pam 212-*ras* line than either cisplatin or acridine. Moreover, compounds **6b** and **6d** showed a preferred activity against the *ras*-transformed cell line compared to the parental line (resistance factor defined as IC_{50} Pam 212-*ras* line/IC_{50} Pam 212 line of 0.3 and 0.5, respectively, versus 1.6 for *cis*-DDP, see Table 1). Thus, the results from the cytotoxicity tests indicate that compounds **6b** and **6d** may be considered good candidates for in vivo antitumour evaluation because they show a good in vitro therapeutic index and are able to circumvent resistance to *cis*-DDP in the cell lines tested.

Because the remarkable cytotoxic properties of compounds **6b** and **6d** may be influenced by their DNA binding ability we have analysed the interaction of both compounds with several DNAs. The results suggest that the fluorescence quenching of ethidium bound to CT DNA on the addition of compounds **6b** and **6d** is caused by the displacement of ethidium from DNA by these bis-intercalators. In addition, the ten times lower C_{50} values obtained for compounds **6b** and **6d** in relation to acridine suggest that they bind more strongly to DNA [12]. On the other hand, pBR322 modification by compounds **6b** and **6d** induces stronger alterations in the mobility of the open circular and covalently closed circular DNA forms relative to acridine. Thus, altogether the DNA binding data indicate that while acridine binds to DNA as a mono-intercalator, compounds **6b** and **6d** act, most likely, as bis-intercalators. In fact, the DNA uncoiling induced by these compounds provides good experimental evidence for such interpretation since compounds **6b** and **6d** show a ϕ value, which is 1.8 times higher than that of acridine.

In summary, the DNA binding experiments reported here suggest that the high cytotoxic activity of compounds **6b** and **6d** may be related to their strong bis-intercalative binding to DNA.

In order to further evaluate the mode of binding of this type of bisintercalators, compound **6d** was selected for molecular modelling studies. As mentioned above, four complexes were constructed and submitted to 100 ps molecular dynamics simulation (see Fig. 4). Results from these simulations were analysed in detail, showing an unexpected trajectory for complex **mA**. As shown in Fig. 6 this complex undergoes remarkable conformational changes in the first 20 ps of the dynamics simulation, demonstrating the marked preference of the chromophores of compound **6d** to bind in a parallel orientation relative to each other and preferentially through the minor groove of the DNA hexamer.

The amount of work devoted to assess the binding mode of monointercalating acridine derivatives has been very extensive including a modelling work carried out by Pindur et al. [15] for amsacrine and related 9-anilino-acridines. In that work it was concluded that all compounds bind by intercalation and some distinct binding modes were observed depending on the substitution pattern. A more recent crystallographic study has solved the structure of a 5-fluoro-9-amino-[26]-acridine-4-carboxamide (5-F-9-amino-DACA) bound to $d(CGTACG)_2$, showing that the drug intercalates between a CpG step and that the protonated dimethylamino chain occupies positions close to N7 and O6 of guanine [13]. However, little work has been carried out in order to understand the binding mode of bisacridine derivatives, and the absence of an X-ray structure of a bis{[(9-oxo-9,10-dihydroacridine-4-carbonyl)amino]-alkyl}alkylamine complexed with DNA justifies a detailed molecular modelling study.

According to the results obtained in this work, compound **6d** prefers to bind locating both chromophores in a parallel orientation, in contrast to other known bisintercalators such as ditercalinium and Flexi-Di [27,28] that bind to DNA orienting its chromophores in an antiparallel orientation.

7. Experimental protocols

7.1. Chemistry

Melting points were determined on a Büchi 530 apparatus and are uncorrected. Thin layer chromatography (TLC) was accomplished using Merck TLC aluminium sheets (silica gel 60 F_{254}). Flash column chromatography was carried out on Merck silica gel (230–400 mesh). All ^{1}H-NMR and ^{13}C-NMR spectra were recorded on a Brucker AM-300 instrument. Chemical shifts are reported as δ values (ppm) downfield from internal Me_4Si in the indicated solvent. The following NMR abbreviations are used: b (broad), s (singlet), d (doublet), t (triplet), q (quartet), m (multiplet), Ar (aromatic proton), ex (exchangeable with D_2O). IR spectra were recorded on a Perkin–Elmer 1330 spectrophotometer and are given in cm^{-1}. Elemental analyses were performed in the Facultad de Farmacia (UCM); all analytical values for C, H and N were within $\pm 0.4\%$ of the theoretical values.

7.1.1. General procedure for the synthesis of 9-oxo-9,10-dihydroacridine-4-carbonyl fluorides (2)

5.0 mmol of cyanuric fluoride were added dropwise to a mixture of 1.0 mmol of the corresponding 9-oxo-9,10-dihydroacridinecarboxylic acid (**1**) and 1.1 mmol of pyridine in anhydrous DMF (15 mL) at 0 °C under argon. The reaction was stirred for 4 h and the solvent eliminated under vacuo. Addition of water (15 mL) followed by extraction with CH_2Cl_2 (3×10 mL) yielded acid fluorides **2** which were used without further purification.

*7.1.1.1. 9-Oxo-9,10-dihydroacridine-4-carbonyl fluoride (**2a**).* Following the general procedure, from 836 mg (3.5 mmol) of 9-oxo-9,10-dihydroacridine-4-carboxylic acid (**1a**), 1.5 mL (17.5 mmol) of cyanuric fluoride and 0.31 mL (3.8 mmol) of pyridine, pure **2a** was obtained as a yellow solid.

^{1}H-NMR (DMSO-d_6) δ 7.36 (t, 1H, $J = 7.3$ Hz, Ar), 7.42 (t, 1H, $J = 8.1$ Hz, Ar), 7.79 (t, 1H, $J = 7.3$ Hz, Ar), 8.22 (d, 1H, $J = 8.1$ Hz, Ar), 8.44 (d, 1H, $J = 7.3$ Hz, Ar), 8.66 (d, 1H, $J = 8.1$ Hz, Ar), 10.95 (s, 1H, NH); IR (KBr) ν 3280 (NH), 1775 (COF), 1630 (CO) cm^{-1}.

*7.1.1.2. 1-Chloro-9-oxo-9,10-dihydroacridine-4-carbonyl fluoride (**2b**).* Following the general procedure, from 465 mg (1.7 mmol) of 1-chloro-9-oxo-9,10-dihydroacridine-4-carboxylic acid (**1b**), 0.7 mL (8.5 mmol) of cyanuric fluoride and 0.15 mL (1.9 mmol) of pyridine, pure **2b** was obtained as a yellow solid.

^{1}H-NMR (DMSO-d_6) δ 7.37 (t, 1H, $J = 7.1$ Hz, Ar), 7.39 (d, 1H, $J = 7.9$ Hz, Ar), 7.78 (t, 1H, $J = 7.1$ Hz, Ar), 7.87 (d, 1H, $J = 8.7$ Hz, Ar), 8.17 (d, 1H, $J = 7.9$ Hz, Ar), 8.30 (d, 1H, $J = 8.7$ Hz, Ar), 11.06 (s, 1H, NH); IR (KBr) ν 3310 (NH), 1745 (COF), 1650 (CO) cm^{-1}.

*7.1.1.3. 1-Nitro-9-oxo-9,10-dihydroacridine-4-carbonyl fluoride (**2c**).* Following the general procedure, from 1.0 g (3.5 mmol) of 1-nitro-9-oxo-9,10-dihydroacridine-4-carboxylic acid (**1c**), 1.5 mL (17.5 mmol) of cyanuric fluoride and 0.31 mL (3.8 mmol) of pyridine, pure **2c** was obtained as a yellow solid.

^{1}H-NMR (DMSO-d_6) δ 7.46 (t, 1H, $J = 8.1$ Hz, Ar), 7.68 (d, 1H, $J = 8.1$ Hz, Ar), 7.88 (t, 1H, $J = 8.1$ Hz, Ar), 8.09 (d, 1H, $J = 8.1$ Hz, Ar), 8.17 (d, 1H, $J = 8.1$ Hz, Ar), 8.62 (d, 1H, $J = 8.1$ Hz, Ar), 11.31 (s, 1H, NH); IR (KBr) ν 3320 (NH), 1770 (COF), 1640 (CO) cm^{-1}.

*7.1.2. Synthesis of 9-oxo-9,10-dihydroacridine-4-carboxylic acid (2-dimethylaminoethyl)amides (**7**)*

*7.1.2.1. 1-Chloro-9-oxo-9,10-dihydroacridine-4-carboxylic acid (2-dimethylaminoethyl)amide (**7b**).* 150 mg (1.70 mmol) of *N*,*N*-dimethylethylenediamine in 0.14 mL (1.70 mmol) of pyridine and 3 mL of DMF were added by dropping to a suspension of 0.47 g (1.70 mmol) of 1-chloro-9-oxo-9,10-dihydroacridine-4-carbonyl fluoride in 6 mL of DMF at room temperature. The resulting mixture was stirred overnight. Elimination of the solvent at reduced pressure, disgregation with a satd. solution of $NaHCO_3$ and chromatography (CH_3OH–NH_4OH 5%) yielded 350 mg (60%) of pure amide as a dark yellow solid. m.p. > 250 °C (dec.)

^{1}H-NMR ($CDCl_3$) δ 2.33 (s, 3H, CH_3), 2.62 (t, 2H, $J = 5.9$ Hz, CH_2), 3.56 (q, 2H, $J = 5.9$ Hz, CH_2), 7.15 (d, 1H, $J = 8.8$ Hz, Ar), 7.24–7.35 (m, 3H, Ar + NH), 7.65 (t, 1H, $J = 7.3$ Hz, Ar), 7.74 (d, 1H, $J = 8.1$ Hz, Ar), 8.40 (d, 1H, $J = 8.1$ Hz, Ar), 12.71 (bs, 1H, NH). ^{13}C-NMR (DMSO-d_6) δ 175.8, 167.3, 143.0, 144.1, 138.9, 137.3, 133.9, 132.6, 126.0, 122.5, 122.3, 121.6, 118.1, 117.4, 116.8, 57.7, 45.1, 37.3; IR (KBr) 3400 (NH), 1640 (CO), 1610 (CO) cm^{-1}. Anal. ($C_{18}H_{18}ClN_3O_2$): C, 62.53; H, 5.43; N, 12.41%.

*7.1.2.2. 1-Nitro-9-oxo-9,10-dihydroacridine-4-carboxylic acid (2-dimethylaminoethyl)amide (**7c**).* 1-Nitro-9-oxo-9,10-dihydro-4-acridinecarboxylic acid (0.69 g, 2.22 mmol) and 1,1′-carbonyldiimidazole (0.78 g, 4.84 mmol) were suspended in DMF (12 mL). The mixture was stirred at room temperature with exclusion of moisture until all solids had dissolved. To the resulting solution cooled at 0 °C was added dropwise 1.00 g (12.10 mmol) of *N*,*N*-dimethylethylenediamine in CH_2Cl_2 (12 mL). The mixture was stirred overnight at room temperature and then diluted with $CHCl_3$, extracted with water and evaporated to yield a crude oil which solidified by stirring in ether. The solid was recrystallized from DMF–ether to give 0.48 g (62%) of pure amide **7c** as a yellow solid. m.p.189–91 °C.

^{1}H-NMR ($CDCl_3$) δ 2.36 (s, 6H, $2 \times CH_3$), 2.66 (t, 2H, $J = 5.5$ Hz, CH_2), 3.61 (m, 2H, CH_2), 7.09 (d, 1H, $J = 7.7$ Hz, Ar), 7.31 (t, 1H, $J = 7.7$ Hz, Ar), 7.39 (d, 1H, $J = 8.2$ Hz, Ar), 7.63 (bs, 1H, NH), 7.70 (td, 1H, $J = 8.0$ Hz, $J = 1.6$ Hz, Ar), 7.98 (d, 1H, $J = 7.7$ Hz, Ar), 8.35 (dd, 1H, $J = 1.0$ Hz, $J = 8.2$ Hz), 12.59 (bs, 1H, NH); ^{13}C-NMR ($CDCl_3$) δ 174.7, 167.0, 151.6, 141.9, 139.4, 134.6, 131.7, 126.9, 123.2, 121.6, 119.8, 117.8, 113.3, 112.6, 57.1, 45.0, 37.2.; IR (KBr) 3440 (CONH), 3280 (NH), 1670 (CO), 1620 (CO) cm^{-1}. Anal. ($C_{18}H_{18}N_4O_4$): C, 59.88; H, 4.89; N, 16.04%.

*7.1.3. General procedure for the synthesis of bis{[(9-oxo-9,10-dihydroacridine-4-carbonyl)amino]alkyl}alkylamines (**3**–**6**)*

A mixture of 1.0 mmol of diamine **7** and 2.0 mmol of pyridine in 4.0 mL of DMF was added to a suspension of the corresponding acid fluoride **2** (2.0 mmol) in 4.0 mL of DMF. The solution was stirred until total reaction (TLC). The crude thus obtained was filtrated and the solvent evaporated under vacuo. The resulting residue was treated with water or a satd. $NaHCO_3$ solution to obtain crude bis{[(9-oxo-9,10-dihydroacridine-4-carbonyl)amino]alkyl}alkylamines **3**–**6**, which was purified by chromatography.

*7.1.3.1. N,N-Bis{2-[(1-chloro-9-oxo-9,10-dihydroacridine-4-carbonyl)amino]ethyl}methylamine (**3b**).* Following the general procedure, 52 mg (0.45mmol) of *N*,*N*-bis(2-aminoethyl)methylamine (**7a**), 0.07 mL (0.9 mmol) of pyridine and 250 mg (0.9 mmol) of 1-chloro-9-oxo-9,10-dihydroacridine-4-carbonyl fluoride (**2b**)

were stirred overnight. Elimination of the solvent at reduced pressure, disgregation with a satd. solution of $NaHCO_3$ and filtration yielded 0.22 g (78%) of pure **3b** after recrystallisation with DMF. m.p. > 250 °C.

^{1}H-NMR (DMSO-d_6) δ 2.44 (s, 3H, CH_3), 2.77 (bs, 4H, 2 × CH_2), 3.51 (bs, 4H, 2 × CH_2), 7.07 (d, 2H, J = 7.9 Hz, Ar), 7.21 (t, 2H, J = 7.1 Hz, Ar), 7.47 (d, 2H, J = 7.9 Hz, Ar), 7.60 (t, 2H, J = 7.9 Hz, Ar), 7.95 (d, 2H, J = 8.7 Hz, Ar), 8.05 (d, 2H, J = 7.9 Hz, Ar), 8.91 (bs, 2H, CONH), 12.68 (bs, 2H, 10-H, ex); ^{13}C-NMR (DMSO-d_6) δ 175.5, 167.4, 142.6, 138.8, 137.4, 133.7, 132.2, 125.9, 122.2, 122.1, 121.5, 117.7, 117.2, 116.4, 55.4, 41.8, 36.9; IR (KBr) ν 3440 (NH), 1640 (CO), 1610 (CO) cm^{-1}; Anal. ($C_{33}H_{27}Cl_2N_5O_4$): C, 62.91; H, 4.57; N, 11.02%.

*7.1.3.2. N,N-Bis{2-[(1-nitro-9-oxo-9,10-dihydroacridine-4-carbonyl)amino]ethyl}methylamine (**3c**).* Following the general procedure, 0.15 mL (1.14 mmol) of *N*,*N*-bis(2-aminoethyl) methylamine (**7a**), 0.18 mL (2.27 mmol) of pyridine and 650 mg (2.27 mmol) 1-nitro-9-oxo-9,10-dihydroacridine-4-carbonyl fluoride (**2c**) were stirred for 4 h. Elimination of the solvent at reduced pressure, disgregation with distilled water and filtration yielded 0.64 g (86%) of pure **3c** after recrystallisation with DMF. m.p. > 250 °C.

^{1}H-NMR (DMSO-d_6) δ 2.45(s, 3H, CH_3), 2.79 (bs, 4H, 2 × CH_2), 3.55 (q, 4H, 2 × CH_2), 7.31–7.36 (m, 2H, Ar), 7.52 (d, 2H, J = 8.1 Hz, Ar), 7.71–7.78 (m, 4H, Ar), 8.11 (d, 2H, J = 8.1 Hz, Ar), 8.24 (d, 2H, J = 8.1 Hz, Ar), 9.12 (bs, 2H, 2 × CONH), 12.51 (bs, 2H, 2 × 10-H, ex); ^{13}C-RMN (DMSO-d_6) δ 173.7; 166.4; 150.4; 140.7; 139.4; 134.6; 133.3; 125.6; 123.0; 121.3; 120.6; 118.6; 113.8; 111.2; 55,6; 41.9; 37.2; IR (KBr) ν 3380 (NH), 1645 (CONH), 1610 (CO) cm^{-1}; Anal. ($C_{33}H_{27}N_7O_8$): C, 61.13; H, 4.26; N, 15.22%.

*7.1.3.3. N,N-Bis{3-[(1-chloro-9-oxo-9,10-dihydroacridine-4-carbonyl)amino]propyl}methylamine (**4b**).* Following the general procedure, 123 mg (0.85 mmol) of *N*,*N*-bis(3-aminopropyl)methylamine (**7b**), 0.14 mL (1.7 mmol) of pyridine, 470 mg (1.7 mmol) of 1-chloro-9-oxo-9,10-dihydroacridine-4-carbonyl fluoride (**2b**) were stirred overnight. Elimination of the solvent at reduced pressure, disgregation with a satd. solution of $NaHCO_3$ and chromatography (CH_3OH–NH_4OH 5%) yielded 300 mg (54%) of pure **4b** as a yellow solid. m.p. > 250 °C (dec.).

^{1}H-NMR ($CDCl_3$) δ 1.91 (bt, 4H, 2 × CH_2), 2.38 (s, 3H, CH_3), 2.67 (bt, 4H, 2 × CH_2), 3.50 (bt, 4H, 2 × CH_2), 6.79 (d, 2H, J = 8.7 Hz, Ar), 7.17–7.27 (m, 4H, Ar), 7.56 (t, 4H, J = 8.7 Hz, Ar), 8.22 (d, 2H, J = 7.9 Hz, Ar), 8.75 (bt, 2H, 2 × CONH), 12.79 (s, 2H, 10-H, ex); ^{13}C-NMR ($CDCl_3$) δ 175.6, 167.3, 142.8, 138.6, 137.3, 133.7, 132.3, 125.9, 122.3, 122.1, 121.5, 117.7, 117.3, 116.4, 54.5, 41.2, 37.6, 25.7; IR (KBr) ν 3400 (NH), 1640 (CONH), 1610 (CO) cm^{-1}; Anal. ($C_{35}H_{31}Cl_2N_5O_4$): C, 64.23; H, 4.91; N, 10.37%.

*7.1.3.4. N,N-Bis{3-[(1-nitro-9-oxo-9,10-dihydroacridine-4-carbonyl)amino]propyl}methylamine (**4c**).* Following the general procedure, 0.18 mL (1.14 mmol) of *N*,*N*-bis(3-aminopropyl) methylamine (**7b**), 0.18 mL (2.27 mmol) of pyridine and 650 mg (2.27 mmol) 1-nitro-9-oxo-9,10-dihydroacridine-4-carbonyl fluoride (**2c**) were stirred for 4 h. Elimination of the solvent at reduced pressure, disgregation with distilled water and filtration yielded 0.63 g (85%) of pure **4c** after crystallisation with DMF. m.p. > 250 °C.

^{1}H-NMR (DMSO-d_6) δ 1.82 (t, 4H, J = 5.9 Hz, 2 × CH_2), 2.32 (s, 3H, CH_3), 2.57 (bs, 4H, 2 × CH_2), 3.43 (t, 4H, J = 5.9 Hz, 2 × CH_2), 7.30–7.35 (m, 2H, Ar), 7.56 (d, 2H, J = 7.3 Hz, Ar), 7.75 (d, 4H, J = 3.7 Hz Ar), 8.11 (d, 2H, J = 8.1 Hz, Ar), 8.28 (d, 2H, J = 7.3 Hz, Ar), 9.27 (bs, 2H, CONH), 12.60 (bs, 2H, 10-H, ex); ^{13}C-NMR (DMSO-d_6) δ 173.7, 166.3, 150.5, 141.1, 139.7, 134.5, 133.2, 125.5, 122.8, 121.2, 120.6, 118.8, 113.8, 111.3, 54.5, 41.3, 37.7, 25.8; IR (KBr) ν 3420 (NH), 1645 (CONH), 1610 (CO) cm^{-1}; Anal. ($C_{35}H_{31}N_7O_8$): C, 62.21; H, 4.77; N, 14.28%.

*7.1.3.5. N,N′-Bis{2-[(1-chloro-9-oxo-9,10-dihydroacridine-4-carbonyl)amino]ethyl}-N,N′-dimethylethylenediamine (**5b**).* Following the general procedure, 63 mg (0.36 mmol) of *N*,*N*′-bis(2-aminoethyl)-*N*,*N*′-dimethylethylenediamine (**7c**), 0.06 mL (0.72 mmol) of pyridine and 200 mg (0.72 mmol) of 1-chloro-9-oxo-9,10-dihydroacridine-4-carbonyl fluoride (**2b**) were stirred for 6 h. Elimination of the solvent at reduced pressure, disgregation with a satd. solution of $NaHCO_3$ and chromatography (CH_3OH–NH_4OH 2%) yielded 150 mg (61%) of pure **5b** as a yellow solid. m.p. 108 °C(dec.).

^{1}H-NMR (DMSO-d_6) δ 2.30 (bs, 6H, 2 × CH_3), 2.56 (bs, 4H, 2 × CH_2), 2.61 (bt, 4H, J = 6.3 Hz, 2 × CH_2), 3.37 (bs, 4H, 2 × CH_2 + H_2O), 7.19–7.28 (m, 4H, Ar), 7.47 (d, 2H, J = 9.5 Hz, Ar), 7.66 (t, 2H, J = 7.9 Hz, Ar), 8.00 (d, 2H, J = 7.9 Hz, Ar), 8.03 (d, 2H, J = 7.9 Hz, Ar), 8.84 (bs, 2H, CONH), 12.81 (bs, 2H, 10-H, ex); ^{13}C-NMR (DMSO-d_6) δ 175.6, 167.2, 142.8, 138.7, 137.4, 133.8, 132.2, 125.9, 122.5, 122.2, 121.5, 117.8, 117.4, 116.3, 55.4, 54.3, 42.3, 37.2; IR (KBr) ν 3350 (b, CONH + NH), 1640 (CONH), 1610 (CO) cm^{-1}; Anal. ($C_{36}H_{34}Cl_2N_6O_4$): C, 62.88; H, 5.02; N, 11.89%.

*7.1.3.6. N,N′-Bis{2-[(1-nitro-9-oxo-9,10-dihydroacridine-4-carbonyl)amino]ethyl}-N,N′-dimethylethylenediamine (**5c**).* Following the general procedure, 300 mg (1.75 mmol) of *N*,*N*′-bis(2-aminoethyl)-*N*,*N*′-dimethylethylenediamine (**7c**), 0.28 mL (3.50 mmol) of pyridine and 1.0 g (3.5 mmol) of 1-nitro-9-oxo-9,10-dihydroacridine-4-carbonyl fluoride (**2c**) were stirred for 2 h. Elimination of the solvent at reduced pressure,

disgregation with a satd. solution of $NaHCO_3$ and chromatography (CH_3OH) yielded 0,7 g (57%) of pure **5c** as a yellow solid. m.p. 218 °C (dec.).

^{1}H-NMR (DMSO-d_6) δ 2.30 (s, 6H, 2 × CH_3), 2.59 (s, 4H, 2 × CH_2), 2.64 (t, 4H, $J = 6.4$ Hz, 2 × CH_2), 3.47 (t, 4H, $J = 6.4$ Hz, 2 × CH_2), 7.27 (t, 2H, $J = 7.9$ Hz, Ar), 7.57 (bs, 2H, CONH), 7.65–7.75 (m, 6H, Ar), 8.01 (d, 2H, $J = 7.9$ Hz, Ar), 8.22 (d, 2H, $J = 8.7$ Hz, Ar), 9.03 (bs, 2H, 10-H, ex); ^{13}C-RMN (DMSO-d_6) δ 173.5, 166.1, 150.5, 141.2, 139.6, 134.2, 132.9, 125.5, 122.5, 121.0, 120.5, 118.7, 113.5, 111.2, 55.4, 54.5, 42.2, 37.3; IR (KBr) ν 3460 (NH), 1670 (CONH), 1640 (C=O) cm^{-1}; Anal. ($C_{36}H_{34}N_8O_8$): C, 61.09; H, 5.11; N, 16.19%.

*7.1.3.7. N,N′-Bis{2-[(9-oxo-9,10-dihydroacridine-4-carbonyl)amino]ethyl}-N,N′-dimethylpropylenediamine (**6a**).* Following the general procedure, 197 mg (1.05 mmol) of *N,N′*-bis(2-aminoethyl)-*N,N′*-dimethylpropylenediamine (**7d**), 0.34 mL (4.18 mmol) of pyridine and 510 mg (2.11 mmol) of 9-oxo-9,10-dihydroacridine-4-carbonyl fluoride (**2a**) were stirred overnight. Elimination of the solvent at reduced pressure, disgregation with a satd. solution of $NaHCO_3$ and chromatography (CH_3OH–NH_4OH 5%) yielded 150 mg (23%) of pure **6a** as a yellow solid. m.p. 130 °C (dec.).

^{1}H-NMR ($CDCl_3$) δ 1.69–1.76 (m, 2H, CH_2), 2.29 (s, 6H, 2 × CH_3), 2.52 (t, 4H, $J = 6.6$ Hz, 2 × CH_2), 2.65 (t, 4H, $J = 5.2$ Hz, 2 × CH_2), 3.54 (q, 4H, $J = 5.2$ Hz, 2 × CH_2), 7.12 (t, 2H, $J = 8.1$ Hz, Ar), 7.20 (t, 2H, $J = 7.3$ Hz, Ar), 7.29 (d, 2H, $J = 7.3$ Hz, Ar), 7.53 (bs, 2H, 2 × CONH), 7.60 (t, 2H, $J = 7.3$ Hz, Ar), 7.90 (d, 2H, $J = 7.3$ Hz, Ar), 8.34 (d, 2H, $J = 8.1$ Hz, Ar), 8.54 (d, 2H, $J = 8.1$ Hz, Ar), 12.26 (s, 2H, 2 × 10-H, ex); ^{13}C-NMR ($CDCl_3$) δ 177.8, 168.2, 141.0, 140.0, 133.7, 131.6, 131.5, 126.7, 122.4, 121.9, 121.1, 119.4, 117.6, 117.3, 55.6, 55.3, 41.6, 36.8, 24.6; IR (KBr) ν 3300 (NH), 1640 (CONH), 1610 (CO) cm^{-1}; Anal. ($C_{37}H_{38}N_6O_4$): C, 70.61; H, 6.22; N, 13.09%.

*7.1.3.8. N,N′-Bis{2-[(1-chloro-9-oxo-9,10-dihydroacridine-4-carbonyl)amino]ethyl}-N,N′-dimethylpropylenediamine (**6b**).* Following the general procedure, 160 mg (0.85 mmol) of *N,N′*-bis(2-aminoethyl)-*N,N′*-dimethylpropylenediamine (**7d**), 0.14 mL (1.7 mmol) of pyridine and 465 mg (1.69 mmol) of 1-chloro-9-oxo-9,10-dihydroacridine-4-carbonyl fluoride (**2b**) were stirred overnight. Elimination of the solvent at reduced pressure, disgregation with a satd. solution of $NaHCO_3$ and chromatography (CH_3OH–NH_4OH 5%) yielded 400 mg (68%) of pure **6b** as a yellow solid. m.p. 175–178 °C.

^{1}H-NMR (DMSO-d_6) δ 1.52–1.63 (m, 2H, CH_2), 2.23 (s, 6H, 2 × CH_3), 2.44 (bt, 4H, 2 × CH_2), 2.56 (bt, 4H, 2 × CH_2), 3.46 (m, 4H, 2 × CH_2 + H_2O), 7.24 (d, 4H, $J = 6.3$ Hz, Ar), 7.54 (d, 2H, $J = 7.9$ Hz, Ar), 7.67 (t, 2H, $J = 7.1$ Hz, Ar), 8.08 (t, 4H, $J = 7.9$Hz, Ar), 8.98 (bs, 2H, 2 × CONH), 12.8 (bs, 2H, 10-H, ex); ^{13}C-NMR (DMSO-d_6) δ 175.5, 167.3, 142.8, 138.6, 137.3, 133.7, 132.3, 125.8, 122.4, 122.0, 121.5, 117.6, 117.3, 116.3, 55.3, 54.7, 41.6, 36.8, 23.5; IR (KBr) ν 3300 (NH), 1640 (CONH), 1610 (CO) cm^{-1}; Anal. ($C_{37}H_{36}Cl_2N_6O_4$): C, 63.79; H, 5.25; N, 11.90%.

*7.1.3.9. N,N′-Bis{2-[(1-nitro-9-oxo-9,10-dihydroacridine-4-carbonyl)amino]ethyl}-N,N′-dimethylpropylenediamine (**6c**).* Following the general procedure, from 330 mg (1.75 mmol) of *N,N′*-bis(2-aminoethyl)-*N,N′*-dimethylpropylenediamine (**7d**), 0.28 mL (3.50 mmol) of pyridine and 1.0 g (3.5 mmol) of 1-nitro-9-oxo-9,10-dihydroacridine-4-carbonyl fluoride (**2c**) were stirred for 3 h. Elimination of the solvent at reduced pressure, disgregation with a satd. solution of $NaHCO_3$ and chromatography (CH_3OH–NH_4OH 2%) yielded 0,8 g (63%) of pure **6c** as a red solid. m.p. 178 °C (dec.).

^{1}H-NMR (DMSO-d_6) δ 1.62 (m, 2H, CH_2), 2.25 (s, 6H, 2 × CH_3), 2.46 (t, 4H, $J = 5.9$ Hz, 2 × CH_2), 2.59 (bt, 4H, 2 × CH_2), 3.45 (bs, 4H, 2 × CH_2), 7.26–7.33 (m, 2H, Ar), 7.53 (d, 2H, $J = 8.1$ Hz, Ar), 7.68–7.76 (m, 6H, 4 × Ar + 2 × CONH), 8.07 (d, 2H, $J = 8.1$ Hz, Ar), 8.28 (d, 2H, $J = 8.1$ Hz, Ar), 9.3 (bs, 2H, 10-H, ex); ^{13}C-NMR (DMSO-d_6) δ 173.5, 166.2, 150.5, 141.3, 139.8, 134.2, 133.0, 125.4, 122.6, 121.2, 120.6, 118.8, 113.5, 111.2, 55.5, 54.9, 41.8, 37.1, 24.0; IR (KBr) ν 3340 (NH), 1640 (CONH), 1610 (CO) cm^{-1}; Anal. ($C_{37}H_{36}N_8O_8$): C, 61.42; H, 5.29; N, 15.38%.

*7.1.4. General procedure for the synthesis of bis{[(1-amino-9-oxo-9,10-dihydroacridine-4-carbonyl)amino]-alkyl}alkylamines (**5d** and **6d**)*

To a suspension of **5c** or **6c** (1.0 mmol) in 25 mL of THF at room temperature, 1.7 g of Raney-Ni (Fluka 83440, suspension in water) and 7.0 mmol of hydrazine monohydrate were added. The crude was stirred for 45 min and the catalyst filtered through celite to obtain, after solvent evaporation and purification by chromatography, pure **5d** and **6d** as yellow solids.

*7.1.4.1. N,N′-Bis{2-[(1-amino-9-oxo-9,10-dihydroacridine-4-carbonyl)amino]ethyl}-N,N′-dimethylethylenediamine (**5d**).* Following the general procedure, from 110 mg (0.15 mmol) of *N,N′*-bis{2-[(1-nitro-9-oxo-9,10-dihydroacridine-4-carbonyl)amino]ethyl}-*N,N′*-dimethylethylenediamine (**5c**), 250 mg of Raney–Ni and 0.05 mL (1.0 mmol) of hydrazine monohydrate, 70 mg (72%) of pure **5d** were obtained, after purification by chromatography ($CHCl_3$–MeOH 50%), as a yellow solid. m.p. 192–195 °C.

^{1}H-NMR ($CDCl_3$) δ 1.60 (bs, 4H, 2 × NH_2), 2.42 (s, 6H, 2 × CH_3), 2.63 (s, 4H, 2 × CH_2), 2.67 (bt, 4H, 2 × CH_2), 3.47 (bs, 4H, 2 × CH_2), 6.03 (d, 2H, $J = 8.7$ Hz, Ar), 7.03–7.13 (m, 6H, 2 × (2-H, Ar + CONH)),

7.31 (d, 2H, $J = 8.7$ Hz, Ar), 7.50 (t, 2H, $J = 7.9$ Hz, Ar), 7.89 (d, 2H, $J = 7.9$ Hz, Ar), 12.74 (bs, 2H, 10-H, ex); ^{13}C-NMR (DMSO-d_6) δ 179.7, 168.6, 155.6, 144.4, 139.2, 133.8, 133.5, 125.5, 121.5, 121.1, 117.4, 105.8, 104.3, 100.3, 56.1, 54.7, 42.5, 37.0; IR (KBr) ν 3380 ($NH + NH_2$), 1630 (CONH), 1600 (CO) cm^{-1}; Anal. ($C_{36}H_{38}N_8O_4$): C, 67.09; H, 6.07; N, 16.99%.

*7.1.4.2. N,N′-Bis{2-[(1-amino-9-oxo-9,10-dihydroacridine-4-carbonyl)amino]ethyl}-N,N′-dimethylpropylenediamine (**6d**).* Following the general procedure, from 110 mg (0.15 mmol) of *N,N′*-bis{2-[(1-nitro-9-oxo-9,10-dihydroacridine-4-carbonyl)amino]ethyl}-*N,N′*-dimethylpropylenediamine (**6c**), 250 mg of Raney–Ni and 0.05 mL (1.0 mmol) of hydrazine monohydrate, 70 mg (70%) of pure **6d** were obtained after purification by chromatography ($CHCl_3$–MeOH 50%), as a yellow solid. m.p. 172–175 °C.

^{1}H-NMR ($CDCl_3$) δ 1.62–1.75 (m, 6H, $2 \times NH_2 + CH_2$), 2.26 (s, 6H, $2 \times CH_3$), 2.48 (t, 4H, $J = 6.6$ Hz, $2 \times CH_2$), 2.59 (t, 4H, $J = 6.0$ Hz, $2 \times CH_2$), 3.47 (q, 4H, $J = 5.5$ Hz, $2 \times CH_2$), 6.11 (d, 2H, $J = 8.8$ Hz, Ar), 6.86 (bs, 2H, $2 \times$ CONH), 7.15 (t, 2H, $J = 7.2$ Hz, Ar), 7.25 (d, 2H, $J = 8.2$ Hz, Ar), 7.47 (d, 2H, $J = 8.2$ Hz, Ar), 7.54 (t, 2H, $J = 8.2$ Hz, Ar), 8.22 (d, 2H, $J = 8.2$ Hz, Ar), 13.18 (bs, 2H, 10-H, ex); ^{13}C-NMR ($CDCl_3$) δ 180.8, 168.9, 155.3, 144.8, 139.4, 133.3, 132.5, 126.0, 121.7, 117.2, 107.0, 104.4, 101.6, 55.9, 55.4, 41.6, 36.5, 24.9; IR (KBr) ν 3380 ($NH + NH_2$), 1630 (CONH), 1600 (CO) cm^{-1}; Anal. ($C_{37}H_{40}N_8O_4$): C, 67.41; H, 6.22; N, 15.84%.

7.2. Biological assays

7.2.1. Biological reagents and compounds

MTT (3-[4,5-dimethylthiazol-2-yl]-2,5-diphenyltetrazolium bromide) was purchased from Sigma Chemical Co. Foetal calf serum (FCS) was supplied by GIBCO-BRL. pBR322 DNA, calf thymus DNA, poly [d(AT)$_2$] and poly [d(GC)$_2$] were obtained from Sigma Co. DDP (cisplatin): *cis*-diamminedichloroplatinum (II), acridine orange hydrochloride and ethidium bromide were also purchased from Sigma Chemical Co. Compounds were dissolved in 15 mM H_3PO_4 in distilled water. Stock solutions of the compounds at concentrations between 0.5 and 1.2 mg mL^{-1} were freshly prepared before use.

7.2.2. Cell lines and culture conditions

Cultures of ovarian carcinoma cell lines sensitive to cisplatin (A2780, CH1) and with acquired resistance to cisplatin (A2780cisR, CH1cisR), normal murine keratinocytes (Pam 212 cells) and murine keratinocytes transformed with H-ras oncogene and resistant to cisplatin (Pam-ras cells) have been described elsewhere [23,25,29].

7.2.3. Drugs cytotoxicity

Cell survival in compound-treated cultures was evaluated by the MTT method as previously reported [30]. Cytotoxicity in human colon cancer cell line HT-29 was carried out as described in previous works [24].

7.2.4. Formation of drug:DNA complexes

Formation of drug:DNA complexes was done by addition to pBR322 DNA (density of supercoiling, $\sigma = -0.067$), CT DNA or poly [d(AT)$_2$] and poly [d(GC)$_2$] oligodeoxynucleotides of aliquots of each compound at different concentrations in 10 mM $NaClO_4$. The amount of compound added to the DNA solution was expressed as r (input molar ratio of drug/nucleotide). The mixture was incubated at 37 °C for various periods of time. The fraction of unreacted drug was separated from the mixture by precipitation of the DNA with 2.5 volumes of ethanol and 0.3 M sodium acetate, pH 4.8.

7.2.5. Fluorescent ethidium displacement assay

Quenching of ethidium–DNA fluorescence by compounds **6b** and **6d** was determined according to previously reported methods [12,31]. Ethidium contains a planar group that intercalates between the stacked bases of DNA [21]. Ultraviolet radiation at 254 nm is absorbed by the DNA and transmitted to intercalated ethidium. This energy is re-emitted at 590 nm in the red–orange region of the visible spectrum. Fluorescence measurements were carried out in a SLM AMINCO-BOWMANN Series S2 luminescence spectrometer coupled to a Hewlett Packard 486 PC. C_{50} values (the μM drug concentration necessary to reduce the fluorescence of initially DNA-bound ethidium by 50%) were obtained using 0.5 μM (in base pairs) of DNA (1.0 mM sodium cacodylate buffer containing 4 mM NaCl, pH 6.0) with 1.26 μM of ethidium at 25 °C. The experiments were repeated four times.

7.2.6. Interaction of compounds **6b** and **6d** with pBR322 plasmid DNA

pBR322 DNA aliquots (50 μg mL^{-1}, density of supercoiling, $\sigma = -0.060$) were incubated with the compounds at 37 °C in TE buffer (Tris–HCl 10 mm, pH 7.4, EDTA 0.1 mM) for 24 h at several molar ratios of drug to nucleotide. The fraction of unreacted drug was separated from the mixture by precipitation of the DNA with 2.5 volumes of ethanol and 0.3 M sodium acetate, pH 4.8. Aliquots of 20 μL of drug:DNA complexes containing 1 μg of DNA were subjected to 1.5% agarose gel electrophoresis for 16 h at 25 V in TAE buffer (40 mM Tris–acetate, 2 mM EDTA, pH 8.0) as previously reported [32,33]. DNA was stained overnight with a TE solution containing 0.5 μg mL^{-1} of ethidium bromide. The experiments were repeated four times.

8. Computational methods

8.1. Model building

Compound **6b** was model-built in Sybyl [34] using standard geometries, which was fully optimised by means of the ab initio quantum mechanical program Gaussian 94 [35] and the STO-3G basis set. Atom-centred point charges for the optimised structure were derived [36] which best reproduced the electrostatic potential of the molecule calculated by means of a single point calculation using the larger 6-31G* basis set. The AMBER [37] all-atom force field parameters [38] were used for the DNA hexamer, and covalent parameters for the intercalating chromophores and linking chain of the ligand were derived, by analogy or through interpolation [39], from those already present in the AMBER database.

The structures of the modelled complexes between $d(GCGCGC)_2$ and Flexi-Di were taken from a previous modelling work [28] and used as a template for modelling the DNA bisintercalation site at two consecutive CpG steps. Models were constructed for the four possible orientations of **6b** relative to the DNA hexamers as shown in Fig. 4.

In order to achieve electrical neutrality in the complexes, an appropriate number of counterions (six) resembling hexahydrated sodium ions were placed in the bisector of the O–P–O groups located further from the positive charges of the ligand [40].

8.2. Energy minimisation

The initial hexamer complexes were refined by progressively minimising their potential energy: first only the counterions and hydrogen atoms were allowed to move; second the interactions between the drug linkers and the central base pairs were optimised; and finally the whole systems were relaxed. Before each minimisation stage, a short optimisation run constraining the atoms to their initial coordinates allowed readjustment of covalent bonds and van der Waals contacts without changing the overall conformation of the complexes. All atom pairs were included in the calculation of the nonbonded interactions. The optimisations were carried out in a continuum medium of relative permittivity $e = 4r_{ij}$ for simulating the solvent environment. For the first 3000 steps of the minimisation all hydrogen bonds between the DNA base pairs, were reinforced with distance and angle restraining functions with force constants of 10 kcal mol^{-1} $Å^{-2}$ and 10 kcal mol^{-1} rad^{-2}, respectively. The optimisations covered a total of about 6000 steps of steepest descent energy minimisation for each of the complexes.

8.3. Molecular dynamics simulations

In order to sample a larger extent of the conformational space, the four lowest energy complexes were subjected to molecular dynamics simulations at 300 K for 100 ps. In a 5 ps heating phase, the temperature was raised in steps of 10 K over 0.1 ps blocks, and the velocities were reassigned at each new temperature according to a Maxwell–Boltzmann distribution. This was followed by an equilibration phase of 15 ps at 300 K, in which the velocities were reassigned in the same way every 0.2 ps and by 80 ps sampling period during which system coordinates were saved every 0.2 ps. The time step used was 1 fs during the heating period and 2 fs for the rest of the simulations. All bonds involving hydrogens were constrained to their equilibrium values by means of the SHAKE algorithm [41], and lists of nonbonded pairs were updated every 25 ps. For the first 30 ps of simulation the atoms of the phosphate–sugar backbone were restrained to their reference positions at 0 ps by means of a harmonic potential with a force constant of 10 kcal mol^{-1} $Å^{-2}$. During the entire simulation time, the G:C hydrogen bonds were reinforced by means of an upper-bound harmonic restraining function with a force constant of 5 kcal mol^{-1} $Å^{-2}$ and 5 kcal mol^{-1} rad^{-1} for distances and angles, respectively.

8.4. Analysis of the dynamics trajectories

Three dimensional structures were visually inspected using the computer graphics program Sybyl [34]. Trajectories were visualised by means of MDDISPLAY [42]. Root-mean-square (rms) deviations from the initial structures and interatomic distances were monitored using CARNAL [37]. Data smoothing for plotting purposes was accomplished by means of routine SMOOFT [43].

9. Conclusions

A series of bis{[(9-oxo-9,10-dihydroacridine-4-carbonyl)amino]alkyl}alkylamines have been prepared and their cytotoxic properties have been tested against HT-29 colon cancer cell lines. The DNA binding experiments reported here suggest that the high cytotoxic activity of compounds **6b** and **6d** may be related to their strong bis-intercalative binding to DNA and molecular dynamics simulations have pointed out that this type of compounds are able to form stable complexes with a model DNA hexamer. According to this modelling study, compound **6b** shows a strong conformational preference to adopt a relative parallel orientation of the chromophores when binding to DNA in contrast to other known bisintercalators such as Ditercalinium and Flexi-Di.

Acknowledgements

This research has been financed in part by the Spanish Comisión Interministerial de Ciencia y Tecnología (PB1998-0055, SAF00-0029) and Universidad San Pablo CEU (USP05/99). Sponsorship by COST Actions D20/0001/00 and D20/0003/00 is kindly acknowledged. C.F. was awarded a "Tercer Premio de Iniciación a la Investigación San Alberto Magno, 1999" for the molecular modelling included in this work. We thank the CIEMAT (Spain) for computer time and facilities and Knoll S.A. for biological activity determinations.

References

[1] L.S. Lerman, Journal of Molecular Biology 3 (1961) 18.
[2] C. Bailly, M. Braña, J. Waring, European Journal of Biochemistry 240 (1996) 195–208.
[3] P.F. Bousquet, M.F. Braña, D. Conlon, K.M. Fitzgerald, D. Perron, C. Cocchiaro, R. Miller, M. Moran, J. George, X.-D. Qian, G. Keilhauer, C.A. Romerdahl, Cancer Research 55 (1995) 1176–1180.
[4] M.F. Braña, J.M. Castellano, M. Moran, M.J. Perez de Vega, D. Perron, D. Conlon, P.F. Bousquet, C.A. Romerdahl, S.P. Robinson, Anti-Cancer Drug Design 11 (1996) 297–309.
[5] M.F. Braña, J.M. Castellano, D. Perron, C. Maher, D. Conlon, P.F. Bousquet, J. George, X.-D. Qian, S.P. Robinson, Journal of Medicinal Chemistry 40 (1997) 449–454.
[6] S.A. Gamage, J.A. Spicer, G.J. Atwell, G.J. Finlay, B.C. Baguley, W.A. Denny, Journal of Medicinal Chemistry 42 (1999) 2383–2393.
[7] S.A. Gamage, J.A. Spicer, G.J. Finlay, A.J. Stewart, P. Charlton, B.C. Baguley, W.A. Denny, Journal of Medicinal Chemistry 44 (2001) 1407–1415.
[8] J.A. Spicer, S.A. Gamage, G.W. Rewcastle, G.J. Finlay, D.J.A. Bridewell, B.C. Baguley, W.A. Denny, Journal of Medicinal Chemistry 43 (2000) 1350–1358.
[9] L.W. Deady, J. Desneves, A.J. Kaye, G.J. Finlay, B.C. Baguley, W.A. Denny, Bioorganic and Medicinal Chemistry 8 (2000) 977–984.
[10] I. Antonini, P. Polucci, L.R. Kelland, E. Menta, N. Pescalli, S. Martelli, Journal of Medicinal Chemistry 42 (1999) 2535–2541.
[11] W.M. Cholody, L. Hernández, L. Hassner, D.A. Scudiero, D.B. Djurickovic, C.J. Michejda, Journal of Medicinal Chemistry 38 (1995) 3043–3052.
[12] Y. Mikata, M. Yokoyama, K. Mogami, M. Kato, I. Okura, M. Chikira, S. Yano, Inorganica Chimica Acta 279 (1998) 51–57.
[13] A. Adams, J.M. Guss, C.A. Collyer, W.A. Denny, A.S. Prakash, L.P.G. Wakelin, Molecular Pharmacology 58 (2000) 649–658.
[14] A.K. Todd, A. Adams, J.H. Thorpe, W.A. Denny, L.P.G. Wakelin, C.J. Cardin, Journal of Medicinal Chemistry 42 (1999) 536–540.
[15] G. Fischer, U. Pindur, Pharmazie 54 (1999) 83–93.
[16] R.M. Wadkins, D.E. Graves, Biochemistry 30 (1991) 4277–4283.
[17] Some of these compounds have been previously described. Antonini I., Martelli S., Polucci P. Bis-acridinecarboxamides having antitumour activity. 1999, WO Patent 9,906,372.
[18] Fieser L.F., Haddadin M.J. (Eds.), Organic Syntheses Collect. Vol. 5; Wiley, New York, 1973.
[19] G.W. Rewcastle, W.A. Denny, Synthesis (1985) 220–222.
[20] L.A. Carpino, E.-S.M.E. Mansour, D. Sadat-Aalaee, Journal of Organic Chemistry 56 (1991) 2611–2614.
[21] J.C. Wang, Journal of Molecular Biology 89 (1974) 783–787.
[22] M.V. Keck, S.J. Lippard, Journal of the American Chemical Society 114 (1992) 3386–3390.
[23] R. Sánchez-Prieto, J.A. Vargas, A. Carnero, E. Marchetti, J. Romero, A. Durantez, J.C. Lacal, S. Ramón y Cajal, International Journal of Cancer 60 (1995) 235–243.
[24] P.F. Bousquet, M.F. Braña, D. Conlon, K.M. Fitzgerald, D. Perron, C. Cocchiaro, R. Miller, M. Morán, J. George, X.D. Qian, G. Keilhauer, C.A. Romerdahl, Cancer Research 55 (1995) 1176–1180.
[25] L.R. Kelland, G. Abel, M.J. McKeage, M. Jones, P.M. Goddard, M. Valenti, B.A. Murrer, K.R. Harrap, Cancer Research 53 (1993) 2581–2586.
[26] A. Adams, J.M. Guss, C.A. Collyer, W.A. Denny, L.P.G. Wakelin, Biochemistry 38 (1999) 9221–9233.
[27] Q. Gao, L.D. Williams, M. Egli, D. Rabinovich, S.L. Chen, G.J. Quigley, A. Rich, Proceedings of the National Academy of Sciences of the United States of America 88 (1991) 2422–2426.
[28] B. de Pascual-Teresa, J. Gallego, A.R. Ortiz, F. Gago, Journal of Medicinal Chemistry 39 (1996) 4810–4824.
[29] L.R. Kelland, C.D.J. Barnard, Drugs of the Future 23 (1998) 1062–1065.
[30] M.C. Alley, D.A. Scudiero, A. Monks, M.L. Hursey, M.J. Czerwinski, D.L. Fine, B.J. Abbott, J.G. Mayo, R.H. Shoemaker, M.R. Boyd, Cancer Research 48 (1988) 589–601.
[31] B.C. Baguley, W.A. Denny, G.W. Atwell, B.F. Cain, Journal of Medicinal Chemistry 24 (1981) 170.
[32] V.M. González, P. Amo-Ochoa, J.M. Pérez, M.A. Fuertes, J.R. Masaguer, C. Navarro-Ranninger, C. Alonso, Journal of Inorganic Biochemistry 63 (1996) 57–68.
[33] A.G. Quiroga, J.M. Pérez, E.I. Montero, J.R. Masaguer, C. Alonso, C. Navarro-Ranninger, Journal of Inorganic Biochemistry 70 (1998) 117–123.
[34] SYBYL, version 6.6., Tripos. St. Louis, Missouri, 1999. http://www.tripos.com
[35] Gaussian 94, revision C. 3., Pople J.A. et al. Gaussian Inc. Pittsburgh, PA, 1995. http://www.gaussian.com
[36] U.C. Singh, P.A. Kollman, Journal of Computational Chemistry 5 (1984) 129.
[37] AMBER, version 5.0, San Francisco, CA, USA, http://www.amber.com
[38] S.J. Weiner, P.A. Kollman, D.T. Nguyen, D.A. Case, Journal of Computational Chemistry 7 (1986) 230–252.
[39] S.J. Weiner, P.A. Kollman, D.A. Case, U.C. Singh, C. Ghio, G. Alagona, S. Profeta, P. Weiner, Journal of the American Chemical Society 106 (1984) 765–784.
[40] F. Gago, C. Reynolds, W.G. Richards, Molecular Pharmacology 35 (1989) 232–241.
[41] J.P. Ryckaert, G. Ciccoti, H.J.C. Berendsen, Journal of Computation and Physics 23 (1977) 327–341.
[42] MDDISPLAY, Version 2.1, Callahan T., Swanson E., Lybrand T., 1994.
[43] Press W.H., Flannery B.P., Teukolsky S.A., Vetterling W.T. (Eds.), Numerical Recipes, Cambridge University Press, Cambridge, UK, 1989.